NeuroImage 54 (2011) 505–516

Contents lists available at ScienceDirect

NeuroImage

journal homepage: www.elsevier.com/locate/ynimg

Effective connectivity anomalies in human amblyopia

Xingfeng Li [a], Kathy T. Mullen [a], Benjamin Thompson [b], Robert F. Hess [a,*]

[a] McGill Vision Research, Department of Ophthalmology, McGill University, 687 Pine Avenue W. (H4-14), Montréal, Quebec, Canada
[b] Department of Optometry and Vision Science, University of Auckland, Auckland, New Zealand

ARTICLE INFO

Article history:
Received 22 February 2010
Revised 22 July 2010
Accepted 24 July 2010
Available online 1 August 2010

Keywords:
fMRI
Amblyopia
Effective functional connectivity
Visual cortex
Human

ABSTRACT

We investigate the effective connectivity in the lateral geniculate nucleus and visual cortex of humans with amblyopia. Six amblyopes participated in this study. Standard retinotopic mapping stimuli were used to define the boundaries of early visual cortical areas. We obtained fMRI time series from thalamic, striate and extrastriate cortical regions for the connectivity study. Thalamo-striate and striate-extrastriate networks were constructed based on known anatomical connections and the effective connectivities of these networks were assessed by means of a nonlinear system identification method. The effective connectivity of all networks studied was reduced when driven by the amblyopic eye, suggesting contrary to the current single-cell model of localized signal reduction, that a significant part of the amblyopic deficit is due to anomalous interactions between cells in disparate brain regions. The effective connectivity loss was unrelated to the fMRI loss but correlated with the degree of amblyopia (ipsilateral LGN to V1 connection), suggesting that it may be a more relevant measure. Feedforward and feedback connectivities were similarly affected. A hemispheric dependence was found for the thalamo-striate feedforward input that was not present for the feedback connection, suggesting that the reduced function of the LGN recently found in amblyopic humans may not be solely determined by the feedback influence from the cortex. Both ventral and dorsal connectivities were reduced.

Introduction

Amblyopia is a disorder of spatial vision, and has been studied extensively using psychophysics, neurophysiology, and brain imaging methods. Brain imaging studies with functional Magnetic Resonance Imaging (fMRI) revealed reduced regional cerebral blood flow and blood-oxygen-level dependent (BOLD) response in the lateral geniculate nucleus (Hess et al., 2009), the striate (Barnes et al., 2001; Conner et al., 2007; Demer, 1997; Demer et al., 1988; Kabasakal et al., 1995; Li et al., 2007) and extra-striate cortex (Barnes et al., 2001; Li et al., 2007; Muckli et al., 2006) in amblyopia. There is also a literature from the numerous psychophysical studies that have been carried out on humans with amblyopia where striate and extra-striate cortical processing anomalies have been inferred. The use of local versus global tasks has helped make inferences about striate versus extra-striate function and the use of spatial (Simmers et al., 2005) versus motion (Aaen-Stockdale and Hess, 2008; Simmers et al., 2003, 2006) stimuli have helped target ventral versus dorsal extra-striate processing. These studies have concluded that both ventral and dorsal extra-striate function is affected in addition to, rather than as a consequence of striate cortical dysfunction. The neural basis of these psychophysical losses are poorly understood because fMRI can only tell us about the function of circumscribed visual cortical areas (segmental view), we have no knowledge of whether the interaction (integrative view) between these areas is normal. To date, the correlation between the fMRI and psychophysical losses has been disappointing (Barnes et al., 2001; Conner et al., 2007; Li et al., 2007; Muckli et al., 2006) and there is a need to obtain another more relevant measure of the cortical dysfunction, one that reflects the interaction between different cortical areas rather than their activation per se. The measure, *effective connectivity* offers just such an assessment (Tononi et al., 1994). Thus to better understand the role played by the interaction between different discrete retinotopically defined cortical areas (i.e. the coordination of different distributed neural populations) in the amblyopic deficit, we assess the effective connectivity in the lateral geniculate nucleus (LGN) and visual cortex of human amblyopes.

Here we use a recently developed nonlinear system identification technique that has previously been validated against more traditional methods (Li et al., 2010) (or appendix). It offers the advantage over Granger Causal Modelling (Roebroeck et al., 2005) of not neglecting non-linear interactions known to occur in the

* Corresponding author. McGill Vision Research, Department of Ophthalmology, McGill University, 687 Pine Avenue W. (H4-14), Montréal, Quebec, Canada H3A 1A1. Fax: +1 514 843 1691.
E-mail address: robert.hess@mcgill.ca (R.F. Hess).

1053-8119/$ – see front matter © 2010 Elsevier Inc. All rights reserved.
doi:10.1016/j.neuroimage.2010.07.053

neural response and the coupling between neural and BOLD responses (Stephan and Friston, 2010). It offers the advantage over Dynamic Causal Modelling (Friston et al., 2003; Stephan et al., 2008) of not requiring a prior structural model. We use this new method for characterizing *effective connectivity* differences *in vivo*, to investigate the directional network interactions between different processing sites in the amblyopic thalamo-cortical pathway. After acquiring brain images (both fMRI and structural MRI) of 6 amblyopes, we defined ROIs for the lateral geniculate and for different cortical areas based on the boundaries of the striate and extra-striate cortex regions (V1 to V4) from the visual field sign maps and diagnostic stimuli. Then we averaged fMRI time series from these regions to assess the functional relationship between different cortical regions.

The critical question is whether the amblyopic deficit involves more than just reduced activation within circumscribed visual areas, as all previous fMRI studies assume (Barnes et al., 2001; Conner et al., 2007; Demer, 1997; Demer et al., 1988; Kabasakal et al., 1995; Li et al., 2007; Muckli et al., 2006). For example, does it also involve anomalous interactions between different visual areas not captured in conventional fMRI measures? Assessment of the effective connectivity between different visual areas can answer this because it relies on causal correlations not instantaneous amplitude measures. If the answer to this question is yes, not only does the current model of the amblyopic deficit in general change (from one involving not only reduced sensitivity but also anomalous interaction) but also a number of questions concerning the nature of these anomalous interactions can be addressed for the first time. For example, is the reduced function of the geniculate due to V1 feedback? Since there is both animal neurophysiological (Chino et al., 1994; Ikeda et al., 1978; Levitt et al., 2001; Sherman et al., 1975; Yin et al., 1997) and human fMRI evidence (Barnes et al., 2001; Hess et al., 2009; Miki et al., 2003) for reduced geniculate and striate function, it is currently unclear whether the primary deficit is in the geniculate (i.e. reduced feedforward) or in the striate cortex (anomalous feedback). Second, since there are deficits to both striate and extra-striate processing, are these effects predominately feedforward or are significant feedback interactions also involved? The extra-striate deficit may follow as a consequence of the striate deficit or, if feedback is increased, visa versa. Finally, is the effective connectivity reduced equally in dorsal and ventral pathways? Previous human psychophysics (Aaen-Stockdale and Hess, 2008; Simmers et al., 2003, 2005, 2006), animal neurophysiology (Kiorpes et al., 2006; Schroder et al., 2002) (Kiorpes et al., 2006; Schmidt et al., 2004) and human fMRI (Barnes et al., 2001; Li et al., 2007) have reported both ventral and dorsal pathway dysfunction. We wanted to know whether the effective connectivity was significantly reduced in both of these pathways.

Materials and methods

Subject and data collection

We studied responses in 6 amblyopes selected to cover a range of etiologies (i.e. 3 strabismic, 1 anisometropic and 2 form-deprivation amblyopes), as detailed in Table 1.

The stimulus was a high-contrast squarewave checkerboard stimulus (check size = 1.5°, field size = 12° width × 10° height) with both AC (i.e. modulated—80% contrast) and DC (i.e. steady- 50 cd/m^2) chromatic and achromatic squarewave modulation at 16 Hz. We referenced responses to a blank with very low luminance (0.1 cd/m2) since most of the cells in the LGN are not DC-balanced and respond to a mean light level. A central black fixation dot was provided throughout all presentations. This was visible, being darker than the background during the blank periods.

Experimental protocols

A standard block design was used composed of alternate stimulus and blank intervals (18 s stimulation, 18 s fixation, 10 blocks per run). Each stimulus was presented in a 2AFC paradigm within a 3-s cycle; each stimulus presentation was for 800 ms with an inter-stimulus interval of 200 ms and 1.2 s for response. To control for attentional modulation known to affect cortical and subcortical structures, subjects performed a 2AFC contrast discrimination task that involved discriminating subtle changes in the contrast of pairs of alternatively presented stimuli within a stimulus cycle and responding with a button press. During the fixation epochs dummy button presses were made. The contrast difference between alternatively presented stimuli was detectable with all subjects performing the task with an average performance of 98.5% ± 2% with the amblyopic eye and 97.8% ± 2% with the fellow fixing eye, demonstrating that the targets were visible to each eye and properly imaged on their retinae. During the experimental paradigm participants viewed the stimuli monocularly and a tight-fitting eye patch was used to fully occlude one eye.

Magnetic resonance Imaging

All magnetic resonance images were acquired using a 4 T Bruker MedSpec system at the Centre for Magnetic Resonance, Brisbane, Australia. A transverse electromagnetic (TEM) head coil was used

Table 1
Clinical details for the six amblyopic participants. The following abbreviations have been used: strab for strabismus; aniso for anisometrope; deprv for deprivation; R for right eye; L for left eye; ET for esotropia; XT for exotropia; HT for hypertropia; ortho for orthotropic alignment; D for dioptre sphere; FIX for monocular fixation; L for left; R for right; CF count fingers.

Subject type	Refractive error	Acuity	Squint	Fixation	Fixation variance	History
JLK	+0.75D	6/5	LET	2° ecc.	±0.74°	Large LET patching age 2 years, surgery age
strabismic	+0.765D	6/48			±2.7°	5 years
BB	+0.50/−0.50x160	6/5	LET	central	±0.39°	Surgery to correct large angle eso age 7
strabismic	+1.00/−0.25x180	6/600			±0.52°	
CRF	−2.75D	6/6	LXT,	4° ecc.	±0.10°	LET and surgery in infancy and age 25 years
strabismic	−3.00D	6/240	LHT		±0.39°	
SJH	+7/−3.00x150	6/30	ortho	central	±0.38°	First Rx
anisomet.	+2.50/−1.25x80	6/4.5			±0.35°	age 19 years
DJL	+8.25/−1.00x90	CF	RET	6° ecc.	±3.1°	2 ops for ET age 9
deprivation	+0.25D	6/6			±0.18°	
MLT	−2.25D	6/6	LXT	2° ecc.	±0.42°	Cataract surgery age 7 years
deprivation	−1.50D	CF			±1.8°	

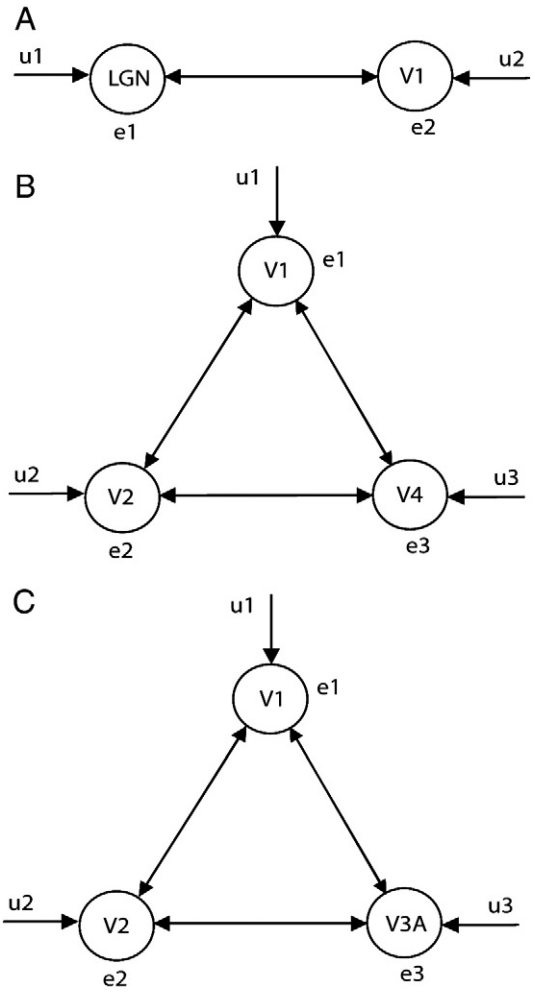

Fig. 1. The three networks examined in the effective connectivity analysis.

for radiofrequency transmission and reception (Vaughan et al., 2002). For the fMRI experimental study, 256 T2*-weighted gradient-echo echoplanar images (EPI) depicting blood oxygen level dependent (BOLD) contrast (Ogawa et al., 1990) were acquired in each of 24 planes with TE 30 ms, TR 1500 ms, in-plane resolution 3.1×3.1 mm and slice thickness 3 mm (0 mm gap). The slices were taken parallel to the calcarine sulcus and arranged to include the anatomical location of the LGN. Two to three fMRI scans were performed in each session. Head movement was limited by foam padding within the head coil. In the same session, a high-resolution 3D T1 image was acquired using an MP-RAGE sequence with TI 1500 ms, TR 2500 ms, TE 3.83 ms, and a resolution of 0.9 mm^3.

Identification of LGN ROI and cortical visual areas

LGN localization was conducted using data collected in a separate scanning session within which the participants were presented with the same stimulus and stimulation parameters described above with the exception that they viewed the stimulus binocularly. Two scanning runs were conducted and t-values for a contrast between fixation vs. stimulation were visualized on each participant's high resolution anatomical scan (transformed to Talairach space). The LGNs were identified as significant regions of activity at the FDR corrected level of $q<0.001$ in the appropriate anatomical location (Hess et al., 2009; Kastner et al., 2004).

To identify cortical visual areas, retinotopic mapping was performed using standard expanding ring and rotating wedge stimuli. Four scanning runs were conducted; clockwise rotating wedge, counter-clockwise rotating wedge, expanding rings and contracting rings. Data were analysed using cross correlation protocols available within Brain Voyager software. Correlation maps for combined polar angle scans (wedge) and the combined eccentricity scans (rings) were visualized on flattened representations of the cortical surface to allow the boundaries between visual areas to be defined. Only voxels within each cortical area that were activated significantly (FDR corrected $q<0.001$) during binocular viewing of the LGN localization stimulus (see above) were included in the cortical ROIs to ensure that non-responsive voxels were excluded.

Data analysis

fMRI data analysis was conducted with the commercially available Brain Voyager analysis package version 1.9.10 (Brain Innovations, Maastricht, The Netherlands). Functional scans were

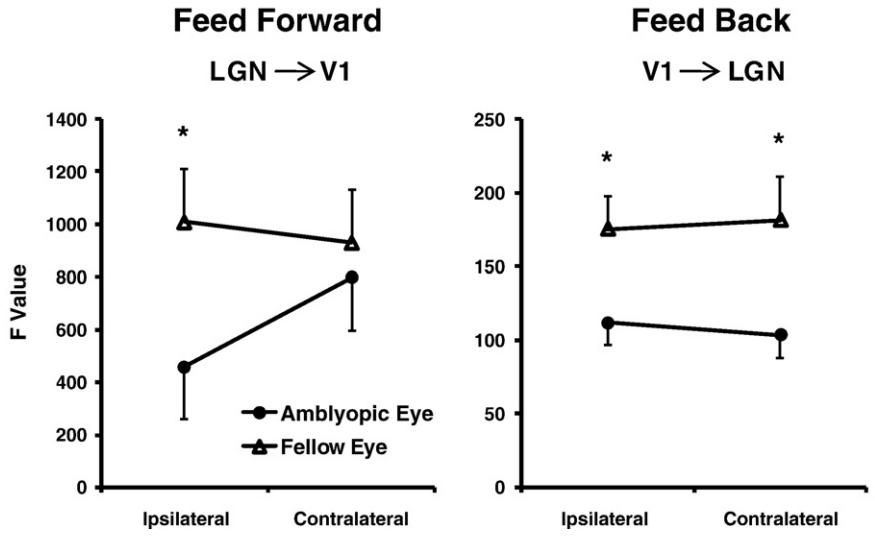

Fig. 2. Effective connectivities for feedforward and feedback lgn/V1 circuit for the fixing and amblyopic eyes of 6 amblyopic humans of different aetiology (see Table 1) quantified in terms of the *F* statistic. Error bars in all data figures show 1SEM across all 12 measurements (2 measurements per eye participant).

Table 2
Statistical evaluation of thalamo-cortical effective connectivity. IL, ipsilateral, CL, contralateral.

Condition	ANOVA: main effect of eye (FDR corrected)	Separate ANOVAs for each hemisphere
Feedforward LGN to V1	$F(1,6)=28.78$, $p=0.002$	IL: $F(1,6)=66.2$, $p<0.001$, CL: $F(1,6)=1.39$, $p=0.28$, non significant
Feedback V1 to LGN	$F(1,6)=14.11$, $p=0.009$	IL: $F(1,6)=10.24$, $p=0.02$, CL: $F(1,6)=13.49$, $p=0.01$.

high-pass filtered and motion corrected using subroutines within Brain Voyager. They were then aligned to each subject's high resolution anatomical images (resampled at 1 mm^3) and transformed to Talairach space (for more details see (Hess et al., 2009)). After this pre-processing, the raw time series data was extracted from each ROI (averaged across all voxels within the ROI) for each scanning run for each participant. This raw time series data formed the basis of the connectivity analysis described below.

The first 12 image volumes were discarded for the connectivity analysis due to start-up instability of the magnetic field, so only 240 image volumes are used in the study. For each early visual cortex region, we averaged all the fMRI response time courses to get one time course for the connectivity study. After obtaining the averaged time course, the time series were normalized temporal by:

$$y(t) = \frac{y_a(t) - \bar{y}}{\mathrm{std}(y_a(t))}$$

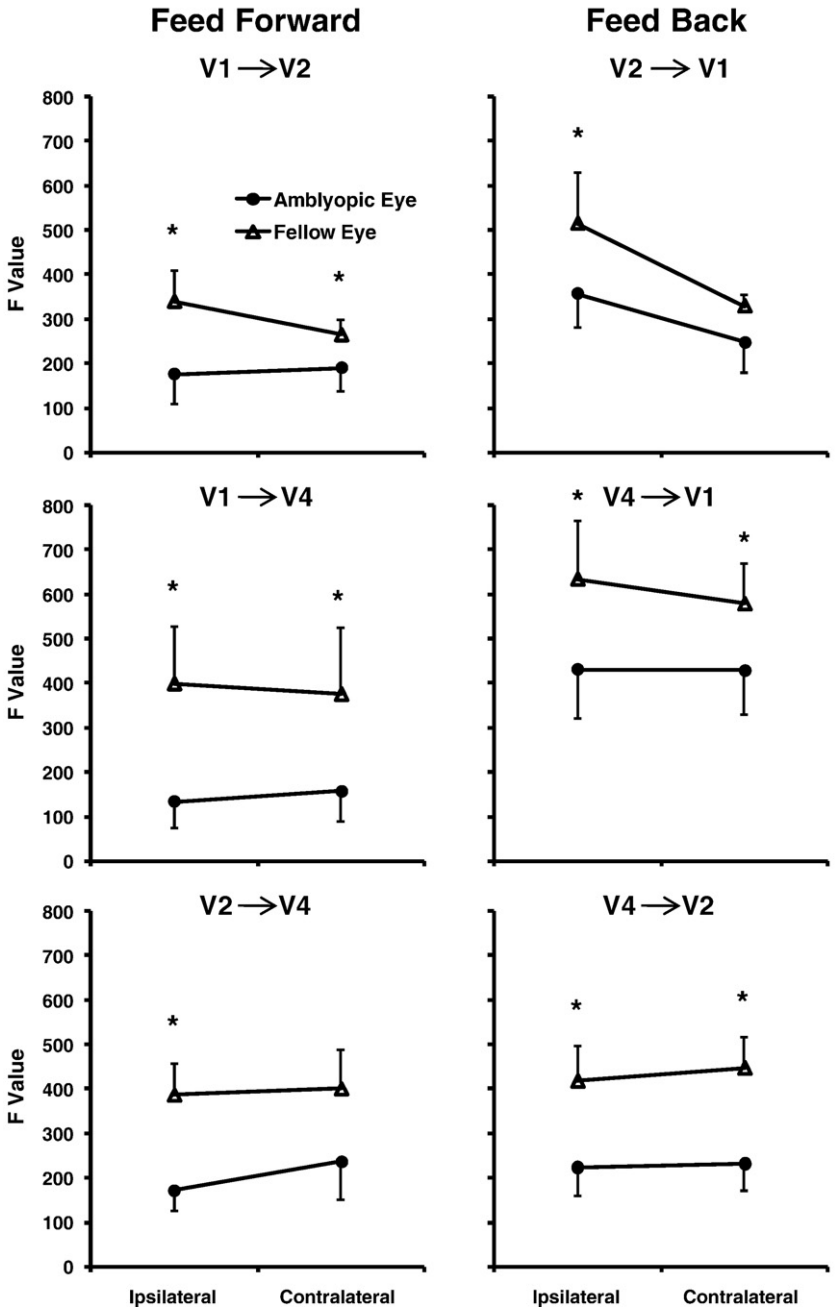

Fig. 3. Effective connectivity results for the ventral cortical stream for the fixing and fellow amblyopic eye of a group of 6 human amblyopes.

where $y_a(t)$is the averaged time series at time t; $\bar{y}$is the mean value of the whole time series $y_a(t)$; $std(y_a(t))$ is the standard deviation of the time series $y_a(t)$.

Nonlinear system identification theory for connectivity study

The physiological processes underlying the BOLD response can be modelled as a multiple-input and multiple-output (MIMO) system (Li et al., 2010):

$$\begin{cases} x(t+1) = f(x(t), u(t), \theta) \\ y(t) = g(x(t), \theta) \end{cases} \quad (1)$$

where f and g are nonlinear functions, and θ represents the set of model parameters. Under some mild assumptions the discrete-time multivariate system (1) with $r1$outputs and $r2$inputs can be described by an autoregressive moving average with exogenous input (NARMAX) as follows (Leontaritis and Billings, 1985a,b):

$$y(t) = f_g\left[y(t-1), \cdots, y\left(t-n_y\right), u(t-1), \cdots, u(t-n_u), e(t-1), \cdots, e(t-n_e)\right] + e(t) \quad (2)$$

where $y(t) = \begin{bmatrix} y_1(t) \\ \vdots \\ y_{r1}(t) \end{bmatrix}, u(t) = \begin{bmatrix} u_1(t) \\ \vdots \\ u_{r2}(t) \end{bmatrix}, e(t) = \begin{bmatrix} e_1(t) \\ \vdots \\ e_{r1}(t) \end{bmatrix}$, are the system output, input and noise, respectively; n_y,n_u, and n_e are the maximum lags in the output, input, and noise; $e(t)$is a zero mean independent sequence; f_g is a new nonlinear function which can be obtained from nonlinear functions f and g. A special case of the general NARMAX model (2) is the nonlinear autoregressive with exogenous inputs (NARX) model:

$$y(t) = f_g\left[y(t-1), \cdots, y\left(t-n_y\right), u(t-1), \cdots, u(t-n_u)\right] + e(t) \quad (3)$$

By applying the regression equation, the NARMAX model (2) and NARX model (3) can be approximated as (Chen et al., 1989; Chon et al., 1997; Zhu and Billings, 1996):

$$y(t) = \sum_{m=0}^{M} W_m(t)\beta_m + e(t),\ t = 0, 1, \cdots, N \quad (4)$$

where $W_0(t) = 1$; for $M \geq 1, W_m(t) = y_1 \Lambda y_i u_1 u_2 \Lambda u_j; i \geq 1; j \geq 0$; m is the number of nonlinear terms; M is the system order; N is the total number of time point in the time series; i is the number of connected regions; j is the number of inputs. Eq. (4) denotes a general case where both input and output terms may be present, but it should be understood that some of the W_m may contain only input or output terms and cross-products or two or more regions (Li et al., 2010). Eq. (4) can be written as an auxiliary system (Edgerton and Shukur, 1999; Kiviet, 1986):

$$Y = W\beta + e \quad (5)$$

where $Y$is $T \times n$,T is the number of time point in the time series, n is the number of output; W is a $T \times K$ linear or nonlinear basis; β is $K \times n$ coefficients matrix; For the error term e, it has $E[e] = 0, E[ee'] = \sigma^2$. The coefficients $\hat{\beta}$ can be obtained by using least squares method in Eq. (5), where the residuals are defined by $\hat{e} = Y - W\hat{\beta}$. Testing connectivity influence or Granger causality (Granger, 1969) between regions is equivalent to test whether columns of W are zero. This can be done by Wald, likelihood ratio (LR), and likelihood multiplier (LM) principle (Engle, 1984). For example, to test whether $\beta_1 = 0$ or not, this can be done by partitioning the coefficients as $\beta = (\beta_1 : \beta_2)$ and $W = (W_1 : W_2)$ accordingly, we can write this test as: $H_0 : \beta_1 = 0$ versus $H_1 : \beta_1 \neq 0$, with the maintained hypothesis given in (5). Defining a R^2-type measures of goodness of fit:

$$R_r^2 = 1 - \left|\hat{e}\hat{e}'\right| \left|\hat{e}_0\ \hat{e}_0\right|^{-1}$$

where $\hat{e}_0$is the residual from regression of Y on W_1 (that is, under H_0; this is the original system), while $\hat{e}$ results from the auxiliary system (5), the corresponding F-approximation to the likelihood-ratio is (Doornik, 1996), Eq. (7)):

$$\text{LMF} = \frac{1 - \left(1 - R_r^2\right)^{1/r}}{\left(1 - R_r^2\right)^{1/r}} \cdot \frac{Nr - q}{np}$$

where $r = \left(\frac{n^2p^2 - 4}{n^2 + p^2 - 5}\right)^{1/2}, q = \frac{1}{2}np - 1, N = T - k - p - \frac{1}{2}(n - p + 1)$, and k is the number of regressors in the original system (k is the column of W_1), n is the dimension of system, T is the number of observations, and $p = ns$(s is the column of W_2). LMF is approximately a $F(np, Ns - q)$distribution (the F-approximation is exact for fixed regressors when $p \leq 2$or $n \leq 2$). When $n = 1$,

$$\frac{R^2}{1 - R^2} \frac{T - k - s}{s} \sim F(s, T - k - s), \quad (6)$$

where $R^2 = \frac{RSS_0 - RSS}{RSS_0}$. RSS_0 and RSS are the residual sum of squares (RSS) of the original and auxiliary system respectively, and $RSS = \sum_{i=1}^{T} e^2(i)$.

Causality test and its application to 2 and 3-connection networks

For the 2-connection network as shown in Fig. 1 (LGN- V1 network) with AR(1) model and second order nonlinearity for example, using $y_1(t)$ and $y_2(t)$ to represent the BOLD response from LGN and V1 respectively. For the model of V1, we have:

$$y_1(t) = a_0 + a_{11}y_1(t-1) + a_{12}y_2(t-1) + a_{13}y_1(t-1)y_2(t-1) - a_{14}y_1(t-1)y_1(t-1) + a_{15}y_2(t-1)y_2(t-1) + a_{16}u_1(t) + e_1(t) \quad (7)$$

Studying the influence of V1 to LGN is equal to test the coefficients before term of $y_2(t-1)$ in the right side of Eq. (7), i.e. a_{12},

Table 3
Statistical evaluation of ventral cortical stream effective connectivity, IL, ipsilateral, CL, contralateral.

Condition	ANOVA: main effect of eye (FDR corrected)	Separate ANOVAs for each hemisphere
Feedforward V1to V2	$F(1,6) = 35.94$, $p = 0.001$	IL: $F(1,6) = 22.64$, $p = 0.003$ CL :$F(1,6) = 15.37$, $p = 0.008$
Feedforward V1 to V4	$F(1,6) = 16.85$, $p = 0.006$	IL: $F(1,6) = 10.70$, $p = 0.02$ CL :$F(1,6) = 21.10$, $p = 0.004$
Feedforward V2 to V4	$F(1,6) = 12.93$, $p = 0.01$	IL: $F(1,6) = 52.36$, $p < 0.001$ CL :$F(1,6) = 4.30$, $p = 0.08$, non significant
Feedback V2 to V1	$F(1,6) = 9.06$, $p = 0.024$	IL: $F(1,6) = 9.25$, $p = 0.02$ CL :$F(1,6) = 5.40$, $p = 0.06$, non significant
Feedback V4 to V1	$F(1,6) = 15.38$, $p = 0.008$	IL: $F(1,6) = 7.64$, $p = 0.033$ CL :$F(1,6) = 23.61$, $p = 0.003$
Feedback V4 to V2	$F(1,6) = 14.61$, $p = 0.009$	IL: $F(1,6) = 6.83$, $p = 0.04$ CL :$F(1,6) = 20.47$, $p = 0.004$

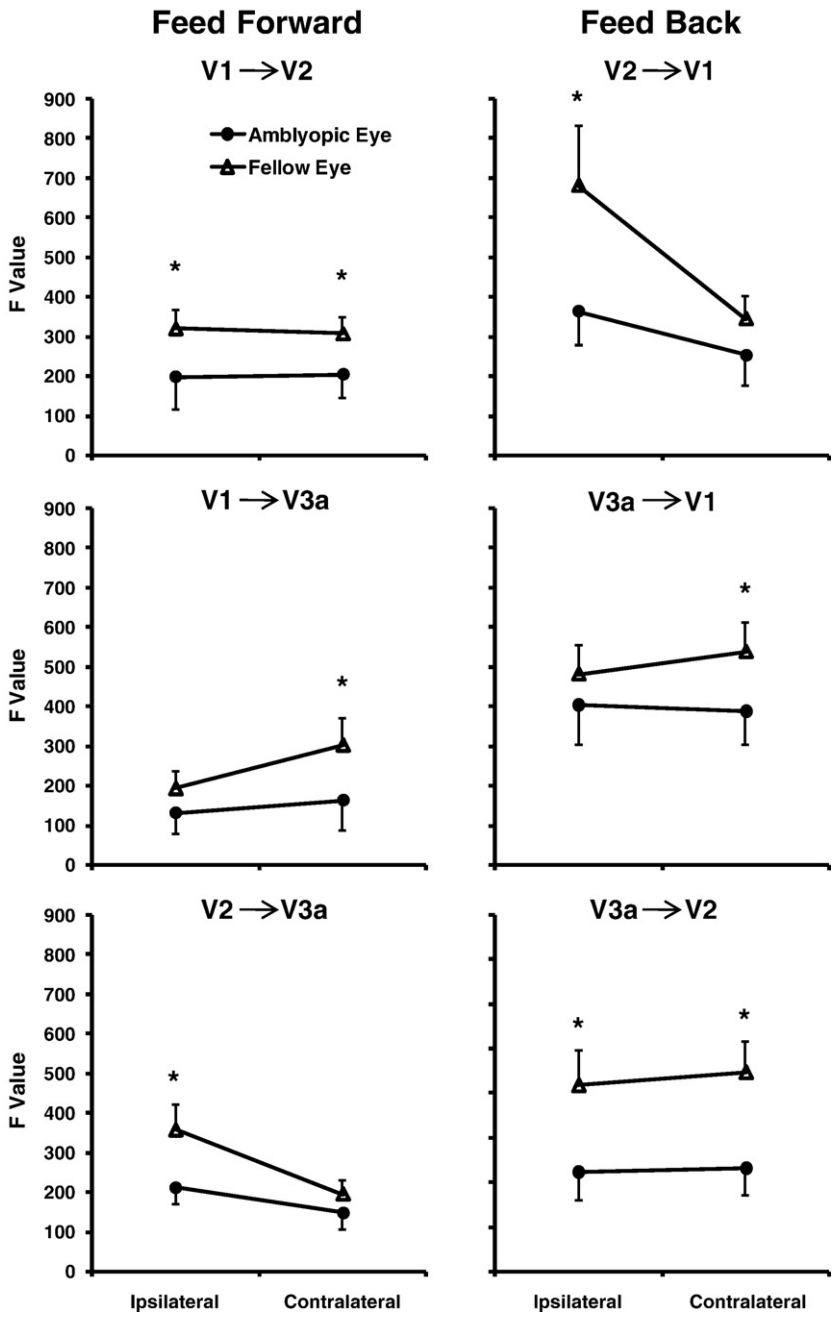

Fig. 4. Effective connectivity results for the Dorsal cortical stream for the fixing and fellow amblyopic eye of a group of 6 human amblyopes.

a_{13}, a_{15} in Eq. (7) to zero. This can be done by using Eq. (6), similarly for the 3-connection network as shown in Fig. 1B (Ventral pathway network). For example, using $y_1(t)$, $y_2(t)$, and $y_3(t)$ to represent the BOLD response from V1, V2v, and V4 respectively. For the model of V1($y_1(t)$) with AR(1) model with second order nonlinearity, we have:

$$\begin{aligned} y_1(t) = {} & a_0 + a_{11}y_1(t-1) + a_{12}y_2(t-1) + a_{13}y_3(t-1) \\ & - a_{14}y_1(t-1)y_1(t-1) + a_{15}y_1(t-1)y_2(t-1) \\ & - a_{16}y_1(t-1)y_3(t-1) + a_{17}y_2(t-1)y_2(t-1) \\ & + a_{18}y_2(t-1)y_3(t-1) + a_{19}y_3(t-1)y_3(t-1) \\ & + a_{20}u_1(t) + e_1(t) \end{aligned} \tag{8}$$

Studying the influence of V2 to V1 is equal to test the coefficients before term of y_2, i.e.a_{12}, a_{15}, a_{17}, a_{18} in Eq. (8) to zero. This can also be done by applying Eq. (6). Using $y_1(t)$, $y_2(t)$, and $y_3(t)$ to represent fMRI response from V1, V2, and V3a respectively, dorsal pathway network influences can be studied in the same way as shown in Eq. (8).

Comparison of effective connectivity for the amblyopic and fellow fixing eyes

Each network quantified connection strength separately for each eye of each subject using the *F*-statistic. To test for differences in effective connectivity between the two eyes, the separate connection strengths for each network were analysed using a mixed ANOVA with within subjects factors of Eye [amblyopic vs. fellow fixing] and Hemisphere [ipsilateral to amblyopic eye vs. contralateral to amblyopic eye] and a between subjects factor of Subject [two fMRI scanning

Table 4
Statistical evaluation of Dorsal cortical stream effective connectivity, IL, Ipsilateral, CL, Contralateral.

Condition	ANOVA: main effect of eye (FDR corrected)	Separate ANOVAs for each hemisphere
Feedforward V1 to V2	$F(1,6)=18.13$, $p=0.005$	IL: $F(1,6)=17.18$, $p=0.006$ CL :$F(1,6)=13.63$, $p=0.01$
Feedforward V1 to V3a	$F(1,6)=13.80$, $p=0.01$	IL: $F(1,6)=3.96$, $p=0.09$, non significant CL :$F(1,6)=7.83$, $p=0.03$
Feedforward V2 to V3a	$F(1,6)=6.31$, $p=0.046$	IL: $F(1,6)=12.96$, $p=0.01$ CL :$F(1,6)=1.31$, $p=0.3$, non significant
Feedback V2 to V1	$F(1,6)=35.14$, $p=0.001$	IL: $F(1,6)=1.89$, $p<0.001$ CL :$F(1,6)=1.31$, $p=0.3$, non significant
Feedback V3a to V1	$F(1,6)=11.68$, $p=0.01$	IL: $F(1,6)=2.59$, $p=0.1$, non significant CL :$F(1,6)=31.80$, $p=0.001$
Feedback V3a to V2	$F(1,6)=23.06$, $p=0.003$	IL: $F(1,6)=12.30$, $p=0.01$ CL :$F(1,6)=29.64$, $p=0.002$

Table 5
Statistical evaluation of Ventral cortical stream effective connectivity without any V1 influence, IL, Ipsilateral, CL, Contralateral.

Condition	ANOVA: main effect of eye (FDR corrected)	Separate ANOVAs for each hemisphere
Feedforward V2 to V4	$F(1,6)=470.34$, $p<0.001$	IL: $F(1,6)=100.07$, $p<0.001$ CL :$F(1,6)=107.55$, $p<0.001$
Feedback V4 to V2	$F(1,6)=50.21$, $p<0.001$	IL: $F(1,6)=9.25$, $p=0.02$ CL :$F(1,6)=9.61$, $p=0.02$

runs per participant]. Degrees of freedom were corrected using the Huhn–Feldt correction. A main effect of Eye was required to demonstrate a difference in the effective connectivity between the two eyes for a pair of visual areas. Since 18 comparisons were tested in total (see below) we used the False Discovery Rate correction proposed by Benjamini and Liu (1999) as implemented in Benjamini et al. (2001) to control for multiple comparisons at this level of the analysis. If a main effect of Eye was found for a particular model, two ANOVAs were conducted (within subject's factor of Eye and between subjects factor of Subject) on the data for the ipsilateral and contralateral hemispheres separately, to investigate whether the difference between the eyes was driven by one hemisphere more that the other.

Results

To better understand the LGN to V1 interactions we determined both the feedforward and feedback effective connectivity for the LGN/V1 circuit (Fig. 1A) when driven by either the fixing or amblyopic eye of our 6 amblyopic subjects. These results are shown in Fig. 2 where we use the F statistic to quantify the connectivity strength for separate ipsi- and contralateral (i.e. to the amblyopic eye) circuits.

The feedforward connections (Fig. 2, left panel) are significantly reduced when driven by the amblyopic eye (Table 2). It is also apparent from Fig. 2 that the majority of the difference between the eyes is carried by the ipsilateral hemisphere (Difference between the eyes for the ipsilateral hemisphere: $F(1,6)=66.2$, $p=0.0002$). This difference is not significant for the contralateral hemisphere ($p=0.3$), showing an ipsilateral/contralateral feedforward effect.

The feedback connectivity (Fig. 2, right panel) is also reduced for the amblyopic eye. A significant main effect of eye was found (Table 2). ANOVAs conducted separately for the two hemispheres demonstrate equivalent significant differences between the eyes for each hemisphere (Table 2), showing that the AE has significantly weaker feedback than that of the FFE for both hemispheres.

The effective connectivity is significantly reduced for the amblyopic eye in all parts of the ventral circuit (Fig. 1B) illustrated in Fig. 3 (significant main effect of Eye, see Table 3 for all statistical values). In terms of the feedforward pathway from V1 to V2 the difference between the two eyes is most pronounced in the ipsilateral hemisphere whereas the contralateral hemisphere shows a smaller effect, however both differences are significant. A similar pattern can be seen for the feedforward pathway from V2 to V4 where the difference between the two eyes is only significant for the ipsilateral hemisphere. The V1 to V4 feedforward pathway showed comparable and significant effects for both hemispheres. For all the feedback interactions the connections driven by the amblyopic eye display reduced effective connectivity from V2 to V1; with only the ipsilateral effects being significant (Table 3), from V4 to V1 and from V4 to V2; significant for both ipsi- and contralateral effects (Table 3).

The feedforward interactions in the Dorsal pathway (Fig. 1D) are also significantly reduced when driven by the amblyopic eye as shown in Fig. 4 (significant main effect of Eye for all models, see Table 4 for statistical values). The reduction in the feedforward interactions from V1 to V2 for the amblyopic eye input is apparent in both hemispheres,

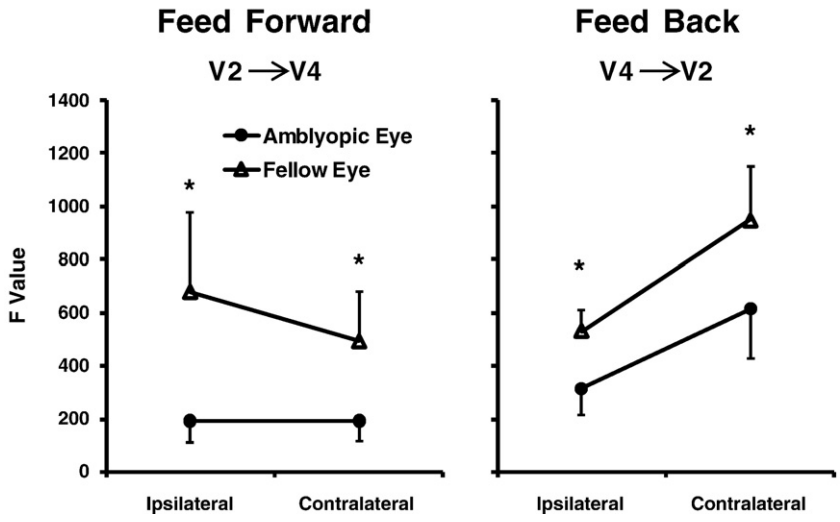

Fig. 5. Ventral interactions after removal of V1.

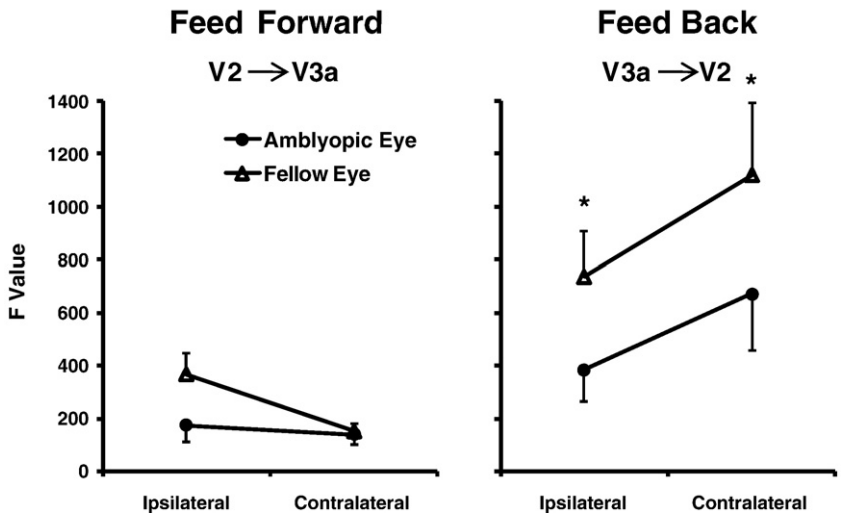

Fig. 6. Dorsal interactions after removal of V1.

whereas the reduction is most pronounced in the contralateral hemisphere for the V1 to V3a interaction and the ipsilateral hemisphere for the V2 to V3a interaction. (Table 4). The feedback effective connectivities are also significantly reduced for the amblyopic eye activation. From V2 to V1, the ipsilateral hemisphere exhibits a significant effect. From V3a to V1, there is a significant effect of eye owing to the statistically significant reduction for the contralateral hemisphere (Table 4). From V3a to V2, effective connectivity is reduced for both hemispheres.

When the influence of V1 is excluded for the ventral pathway (see Fig. 1C), the effective connectivity is significantly reduced for both hemispheres for both the feedforward and feedback interactions, as shown in Fig. 5 (Table 5).

When the influence of V1 is excluded for the dorsal pathway (Fig. 1 E), the feedforward effective connectivity is significantly reduced overall (significant main effect of eye) however neither hemisphere shows a significant effect when considered alone (although the effect for the ipsilateral hemisphere is marginal ($p = 0.054$). The feedback interactions are significantly reduced for both hemispheres, as shown in Fig. 6 (Table 6).

Discussion

This is the first report of effective connectivity along the visual pathway of humans with amblyopia. It allows us to answer a number of presently unresolved questions concerning the neurological deficit. We know from fMRI that a number of sites along the thalamo-cortical pathway are less responsive, this includes the lateral geniculate nucleus (Hess et al., 2009; Miki et al., 2003), the striate cortex (Conner et al., 2007; Demer, 1997; Demer et al., 1988; Kabasakal et al., 1995) and ventral and dorsal extrastriate visual areas (Barnes et al., 2001; Li et al., 2007; Muckli et al., 2006). However fMRI studies tell us nothing about the interactions that occur between these various processing sites. For example, does the amblyopic anomaly involve only cells that are less responsive in circumscribed brain regions or are there also anomalous interactions between different brain regions? If the latter is the case then our model of amblyopia should include not only cellular signal reduction in localized cortical areas but also anomalous interaction between cells in disparate brain regions. If so, the nature of these anomalous interactions between different brain areas needs to be assessed. For example, are feedforward and feedback interactions equally affected? These are important questions that bear upon an understanding of the recently reported geniculate fMRI deficit in amblyopia (Hess et al., 2009) as well as the inter-relationship between the striate and extrastriate deficits in amblyopia.

We show that the effective connectivity is reduced for vision through the amblyopic eye. This interaction deficit occurs between all visual sites tested and is present for both feedforward and feedback transmission. This is the first evidence of a deficit involving the interaction between neurons in disparate brain regions in amblyopia, in other words a deficit of integrative brain function (Tononi et al., 1994). Since fMRI signals from the fixing and amblyopic eye were normalized prior to the calculation of effective connectivity, we would not expect these reductions in effective connectivity to the direct result of reduced BOLD activation. Additionally, we find no significant correlation between the fMRI and effective connectivity cortical deficits in our amblyopic group, suggesting they reflect different aspects of cortical dysfunction. Table 7 shows the correlations between these two measures for visual areas in the dorsal and ventral

Table 6
Statistical evaluation of Dorsal cortical stream effective connectivity without any V1 influence, IL, ipsilateral, CL, contralateral.

Condition	ANOVA: main effect of eye (FDR corrected)	Separate ANOVAs for each hemisphere
Feedforward V2 to V3a	$F(1,6) = 7.50$, $p = 0.03$	IL: $F(1,6) = 5.72$, $p = 0.054$, non significant CL : $F(1,6) = 0.84$, $p = 0.8$, non significant
Feedback V3a to V2	$F(1,6) = 121.31$, $p < 0.001$	IL: $F(1,6) = 11.68$, $p = 0.01$ CL : $F(1,6) = 23.26$, $p = 0.003$

Table 7
Correlation between fMRI % BOLD deficits and effective connectivity deficits in the cortical areas comprising the dorsal and ventral cortical networks described in Fig. 1. The $df = 7–2$; critical r value $= 0.75$ ($p < 0.05$).

from:	To: V1	V2	V3A	V4
V1		0.56	0.16	0.57
V2	−0.41		0.47	0.21
V3A	−0.72	0.39		
V4	−0.61	0.44		

circuits investigated. Interestingly, we find a correlation between the connectivity deficit (FFF connectivity-AME connectivity) and the behavioural acuity deficit for a number of visual areas. The bigger the difference between AME and FFE ipsilateral connectivity, the worse the AME acuity. Significant effects are observed for LGN to V1 (Rho (6) = −0.928, $p = 0.008$), V2 to V1(Rho (6) = 0.812, $p = 0.05$), V1 to V4 (Rho (6) = 0.812, $p = 0.05$), and V3a to V2 (Rho (6) = 0.812, $p = 0.05$) when V1 is not included in the model. However it should be noted that only the V1 to LGN ipsilateral correlation remains significant when corrections for multiple comparisons within each model are imposed. All the comparisons that show significant correlations also show significant differences between the two eyes. This is all the more interesting since fMRI studies (Barnes et al., 2001; Li et al., 2007; Muckli et al., 2006) have not been able to find significant correlations between the reduced activations of these defined visual areas and the acuity deficit. Thus effective connectivity is telling us something different from fMRI and what's more it appears to be related to the behavioural loss.

These results allow us to answer a number of questions about the nature of this integrative loss.

Is the reduced function of the Geniculate due to V1 feedback?

The results suggest that the poor response of the geniculate may not be able to be completely accounted for in terms of cortical feedback because the feedforward anomaly in effective connectivity shows an ipsilateral/contralateral to amblyopic eye bias not present in the feedback, suggesting a thalamic deficit per se. It is interesting to note that while we found no ipsilateral/contralateral fMRI bias for these subjects (Hess et al., 2009), the only human post mortem study has shown that there is greater cell shrinkage for the geniculate ipsilateral to the amblyopic eye (von Noorden and Crawford, 1992). Are these effects predominately feedforward or are significant feedback interactions involved? We show that feedforward and feedback anomalies occur in effective connectivity for all sites tested, suggesting that anomalous feedback from extrastriate to striate cortex is not the sole cause of amblyopia. Is the effective connectivity reduced equally in dorsal and ventral pathways? We find effective connectivity deficits for both ventral and dorsal pathways of approximately the same magnitude. Is the extrastriate deficit solely a consequence of reduced input from striate cortex? We find anomalous interactions between all cortical areas, not just those involving area V1. Furthermore, when we exclude the influence of V1, the anomalous interactions remain between other visual areas in both ventral and dorsal pathways, suggesting primary deficits in extra-striate cortex. The conclusions above are not determined by our use of discrete ventral and dorsal circuit models because we also analysed the connectivities between fixing and amblyopic eye stimulation for the same areas in a large scale model (Fig. 1 Appendix B) where all areas were interconnected and found similar results (see Figs. 2 and 3 Appendix B).

Although at this stage the reason for the reduced effective connectivity throughout the visual pathway driven by the amblyopic eye is unclear a number of obvious explanations can be ruled out. We do not think it is due to differences in HRF between the fixing and amblyopic eyes because we used a standard block design and Fourier methods. The former would not be particularly susceptible to HRF effects (compared with an event-related design) and the latter would adaptively model any differences that might exist. Another worry is whether the piecemeal way we have assessed the effective connectivity of the fixing and amblyopic eyes in three separate but essentially overlapping circuits may have influenced the outcome. In the appendix we present results for a single model simulation involving all visual structures. The results support our main finding showing reduced effective connectivity for amblyopic eye inputs.

We were able to simulate reductions in effective connectivity by adding extra neural noise to the fMRI signal from the fixing eye activation. This is however not a good model (i.e. additive, zero mean noise) of the fMRI deficit in amblyopia because the fMRI deficits are not just more noisy (e.g. Li et al., 2007), suggesting that the effective connectivity and fMRI deficits have separate causes.

In summary, it has been tempting in the past to try to assign certain visual deficits in amblyopia to particular circumscribed visual cortical areas without considering the possibility that they could be due to a disruption in the communication between a number of different cortical areas. Brain function involves an interplay between segregative and integrative functions (Tononi et al., 1994) to allow the cooperative activity of distributed neuronal populations to encode specific behavioural states. It has previously been shown using fMRI by us (Barnes et al., 2001; Hess et al., 2009; Li et al., 2007) and others (Conner et al., 2007; Demer, 1997; Demer et al., 1988; Kabasakal et al., 1995; Miki et al., 2003; Muckli et al., 2006) that the responsiveness of different visual cortical areas and thalamic sites is reduced in amblyopia. Here we show that the interaction, both feedforward and feedback is anomalous in amblyopia, that this deficit extends throughout the thalamo-cortical pathway, it occurs in addition to the regional fMRI loss and it correlates with the behavioural loss.

Acknowledgments

This work was supported by a CIHR grants (#MOP53346) to RFH and (#MOP-10819) to KTM and to a grant from the Wesley Research institute, Brisbane.

Appendix A. noise simulation model for reduced connectivity

Simulation parameters: std = 0.2 Gaussian noise (mean = 0).

Input data: fMRI data from the fixing eye of subject BB, Gaussian noise (std = 0.2) was added and repeated 1000 times. The results are as follows:

Original data for the fixing eye: influence from V2 to V1 is 566.0600 (P<0.05); influence from V4 to V1 is 260.9235 (P<0.05).

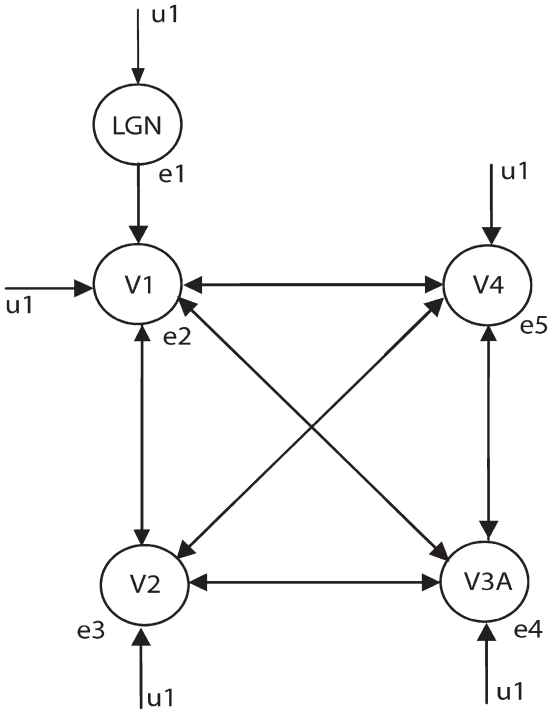

Fig. 1 Appendix B. Details of the large scale model.

After additive the noise, the mean value of influence from V2 to V1 is 101.4810 with standard deviation of 12.0246. The mean value of influence from V4 to V1 is 106.0067 ($P<0.05$).

In Summary, reduced connectivity can be simulated by a reduced signal/noise ratio in the neural signal

Appendix B. Large scale model results

An analysis of connectivity strength using a large model (Fig. 1. Appendix B) that included all visual areas confirmed our previous finding from piecemeal models that the amblyopic eye connectivity was significantly weaker than the fellow eye connectivity in both the ventral and dorsal steam (Figs. 2 Appendix B and 3 Appendix B). ANOVA analysis (FDR corrected for multiple comparisons) confirmed a main effect of eye for all the connections tested. ANOVAs (Table 1 Appendix B) run separately for each hemisphere showed that this main effect was driven by both ipsilateral (to the amblyopic eye) and contralateral connectivity loss for the amblyopic eye, with the exception of the V1 to V4 connection where the loss was driven mainly by the contralateral connections. Connectivity between the

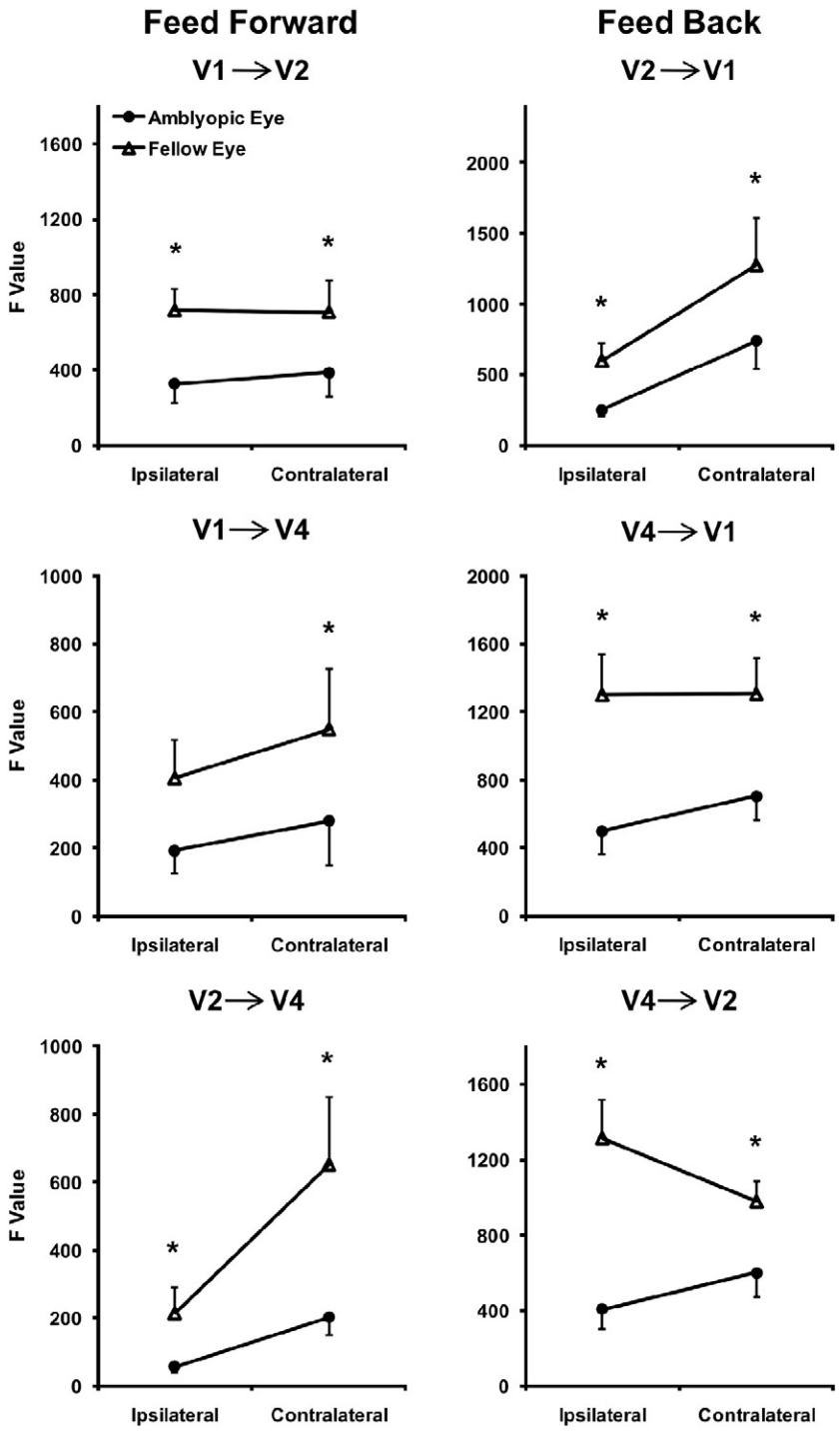

Fig. 2 Appendix B. Connectivities for fixing (open triangles) and amblyopic (filled circles) eye stimulation the ventral circuit of the large scale model.

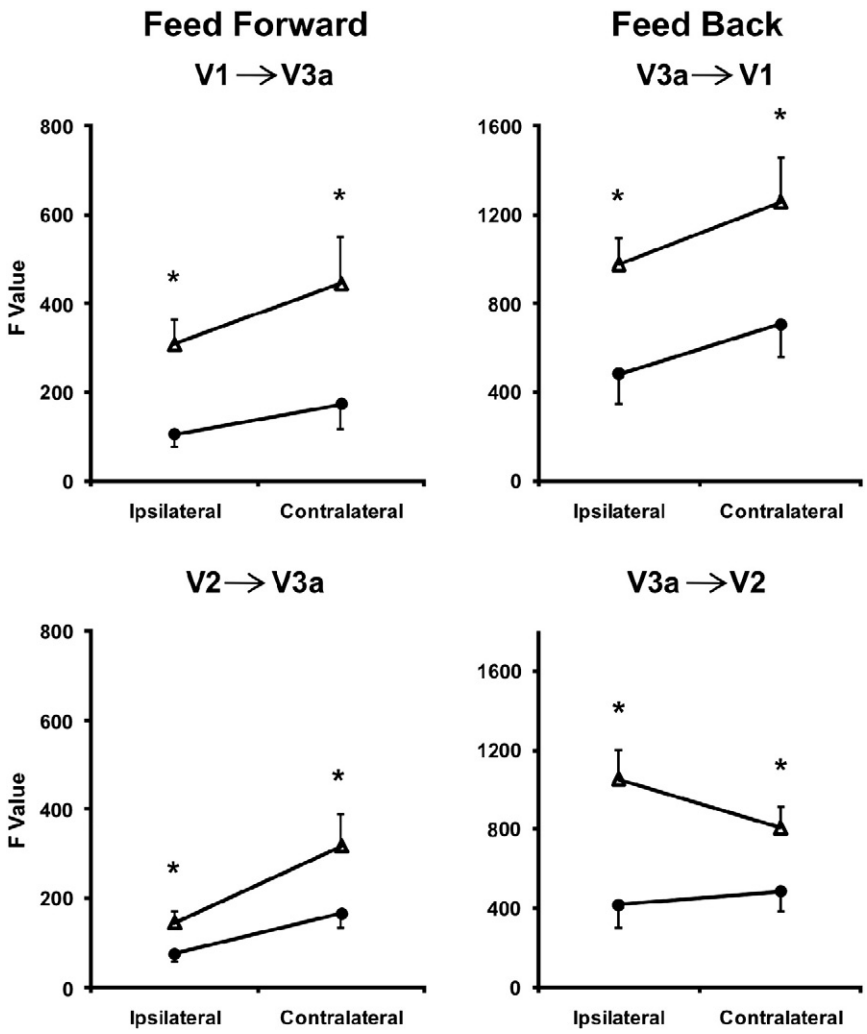

Fig. 3 Appendix B. Connectivities for fixing (open triangles) and amblyopic (filled circles) eye stimulation for the dorsal circuit of the large scale model.

LGN and V1 did not differ between this large model and the previous piecemeal analysis reported above. Statistical values for the comparisons are shown below.

Table 1 Appendix B
Results of ANOVAs for large scale circuit analysis.

Condition	ANOVA: main effect of eye (FDR corrected)	Separate ANOVAs for each hemisphere
Feedforward V1 to V2	$F(1,6) = 28.60$, $p = 0.002$	IL: $F(1,6) = 20.17$, $p = 0.004$ CL: $F(1,6) = 13.75$, $p = 0.01$
Feedforward V1 to V4	$F(1,6) = 11.70$, $p = 0.01$	IL: $F(1,6) = 4.46$, $p = 0.06$ non-significant CL: $F(1,6) = 24.31$, $p = 0.003$
Feedforward V2 to V4	$F(1,6) = 36.69$, $p = 0.001$	IL: $F(1,6) = 8.48$, $p = 0.03$ CL: $F(1,6) = 61.53$, $p < 0.001$
Feedforward V1 to V3a	$F(1,6) = 25.00$, $p = 0.002$	IL: $F(1,6) = 19.10$, $p = 0.005$ CL: $F(1,6) = 17.31$, $p = 0.006$
Feedforward V2 to V3a	$F(1,6) = 34.57$, $p = 0.001$	IL: $F(1,6) = 7.43$, $p = 0.03$ CL: $F(1,6) = 25.92$, $p = 0.002$
Feedback V2 to V1	$F(1,6) = 11.96$, $p = 0.01$	IL: $F(1,6) = 10.36$, $p = 0.02$ CL: $F(1,6) = 11.63$, $p = 0.01$
Feedback V4 to V1	$F(1,6) = 40.62$, $p < 0.001$	IL: $F(1,6) = 71.45$, $p < 0.001$ CL: $F(1,6) = 116.26$, $p < 0.001$
Feedback V4 to V2	$F(1,6) = 41.80$, $p = 0.001$	IL: $F(1,6) = 141.14$, $p < 0.001$ CL: $F(1,6) = 31.00$, $p < 0.001$
Feedback V3a to V1	$F(1,6) = 24.37$, $p < 0.001$	IL: $F(1,6) = 24.07$, $p = 0.003$ CL: $F(1,6) = 207.28$, $p < 0.001$
Feedback V3a to V2	$F(1,6) = 76.23$, $p < 0.001$	IL: $F(1,6) = 98.28$, $p < 0$ 001 CL: $F(1,6) = 37.43$, $p = 0.001$

Appendix C. Supplementary data

Supplementary materials related to this article can be found online at doi:10.1016/j.neuroimage.2010.07.053.

References

Aaen-Stockdale, C., Hess, R.F., 2008. The amblyopic deficit for global motion is spatial scale invariant. Vis. Res. 48, 1965–1971.
Barnes, G.R., Hess, R.F., Dumoulin, S.O., Achtman, R.L., Pike, G.B., 2001. The cortical deficit in humans with strabismic amblyopia. J. Physiol. (Lond) 533, 281–297.
Benjamini, Y., Drai, D., Elmer, G., Kafkafi, N., Golani, I., 2001. Controlling the false discovery rate in behavior genetics research. Behav. Brain Res. 125, 279–284.
Benjamini, Y., Liu, W., 1999. A step-down multiple hypothesis testing procedure that controls the false discovery rate in multiple comparison problems. J. Stats Plann. Inference 82, 1–2.
Chen, S., Billings, S.A., Luo, W., 1989. orthogonal least squaresmethods and their application to non-linear system identification. Int. J. Control 50, 1873–1896.
Chino, Y.M., Smith III, E.L., Yoshida, K., Cheng, H., Hamamoto, J., 1994. Binocular interactions in striate cortical neurons of cats reared with discordant visual inputs. J. Neurosci. 14, 5050–5067.
Chon, K., Korenberg, M.J., Holstein-Rathluo, N.H., 1997. Application of fast orthogonal search to linear and non-linear stochastic systems. Ann. Biomed. Eng. 25, 793–801.
Conner, I.P., Odom, J.V., Schwartz, T.L., Mendola, J.D., 2007. Monocular activation of V1 and V2 in amblyopic adults measured with functional magnetic resonance imaging. J. AAPOS 11, 341–350.
Demer, J.L., 1997. Positron-emission tomographic study of human amblyopia with use of defined visual stimuli. J. AAPOPS 1, 158–171.
Demer, J.L., von Noorden, G.K., Volkow, N.D., Gould, K.L., 1988. Imaging of cerebral flow and metabolism in amblyopia by positron emission tomography. Am. J. Ophthalmol. 105, 337–347.

Doornik, J.A., 1996. Testing vector error autocorrelation and heteroscedasticity. Econometric Society 7th Congress, Tokyo.
Edgerton, D., Shukur, G., 1999. Testing autocorrelation in a system perspective testing autocorrelation. Econometric Rev. 18, 343–386.
Engle, R.F., 1984. Wald likelihood ratio and Lagrange Multiplier tests in econometrics. Handbook of Econometricism, vol. II, pp. 775–826.
Friston, K.J., Harrison, L., Penny, W., 2003. Dynamic causal modelling. Neuroimage 19, 1273–1302.
Granger, C., 1969. Investigating causal relations by econometric data and cross spectral methods. Econometrica 37, 424–438.
Hess, R.F., Thompson, B., Gole, G., Mullen, K.T., 2009. Deficient responses from the lateral geniculate nucleus in humans with amblyopia. Eur. J. Neurosci. 29, 1064–1070.
Ikeda, H., Tremain, K.E., Einon, G., 1978. Loss of spatial resolution of lateral geniculate nucleus neurones in kittens raised with convergent squint produced at different stages of development. Exp. Brain Res. 31, 207–220.
Kabasakal, L., Devranoglu, K., Arslan, O., Erdil, T.Y., Sonmezoglu, K., Uslu, I., Tolunm, H., Isitman, A.T., Ozker, K., Onsel, C., 1995. Brain SPECT evaluation of the visual cortex in amblyopia. J. Nucl. Med. 36, 1170–1174.
Kastner, S., O'Connor, D.H., Fukui, M.M., Fehd, H.M., Herwig, U., Pinsk, M.A., 2004. Functional imaging of the human lateral geniculate nucleus and pulvinar. J. Neurophysiol. 91, 438–448.
Kiorpes, L., Tang, C., Movshon, J.A., 2006. Sensitivity to visual motion in amblyopic macaque monkeys. Vis. Neurosci. 23, 247–256.
Kiviet, J.F., 1986. On the rigor of some misspecification tests for modelling dynamic relationships. Rev. Econom. Stud. 53, 241–261.
Leontaritis, I., Billings, S.A., 1985a. Input–output parametric models for non-linear systems. Part I deterministic non-linear systems. Int. J. Control 41, 303–328.
Leontaritis, I., Billings, S.A., 1985b. Input–output parametric models for non-linear systems. Part II stochastic non-linear systems. Int. J. Control 41, 329–344.
Levitt, J.B., Schumer, R.A., Sherman, S.M., Spear, P.D., Movshon, J.A., 2001. Visual response properties of neurons in the LGN of normally reared and visually deprived macaque monkeys. J. Neurophysiol. 85, 2111–2129.
Li, X., Dumoulin, S.O., Mansouri, B., Hess, R.F., 2007. Cortical deficits in human amblyopia: their regional distribution and their relationship to the contrast detection deficit. Invest. Ophthal. Vis. Sci. 48, 1575–1591.
Li, X., Marrelec, G., Hess, R.F., Benali, H., 2010. A nonlinear identification method to study effective connectivity in functional MRI. Med. Image Anal. 14, 30–38.
Miki, A., Liu, G.T., Goldsmith, Z.G., Haselgrove, J.C., 2003. Decreased activation of the lateral geniculate nucleus in a patient with anisometropic amblyopia demonstrated by functional magnetic resonance imaging. Ophthalmologica 217, 365–369.
Muckli, L., Kiess, S., Tonhausen, N., Singer, W., Goegel, R., Sireteanu, R., 2006. Cerebral correlates of impaired grating perception in individual psychophysically assessed human amblyopes. Vis. Res. 46, 506–526.
Ogawa, S., Lee, T.M., Kay, A.R., Tank, D.W., 1990. Brain magnetic resonance imaging with contrast dependent on blood oxygenation. Proc. Natl Acad. Sci. USA 87, 9868–9872.
Roebroeck, A., Formisano, E., Goebel, R., 2005. Mapping directed influence over the brain using Granger causality and fMRI. Neuroimage 25, 230–242.
Schmidt, K.E., Singer, W., Galuske, R.A., 2004. Processing deficits in primary visual cortex of amblyopic cats. J. Neurophysiol. 91, 1661–1671.
Schroder, J.H., Fries, P., Roelfsema, P.R., Singer, W., Engel, A.K., 2002. Ocular dominance in extrastriate cortex of strabismic amblyopic cats. Vis. Res. 42, 29–39.
Sherman, S.M., Wilson, J.R., Guillery, R.W., 1975. Evidence that binocular competition affects the postnatal development of Y-cells in the cat's lateral geniculate nucleus. Brain Res. 100, 441–444.
Simmers, A.J., Ledgeway, T., Hess, R.F., 2005. The influences of visibility and anomalous integration processes on the perception of global spatial form versus motion in human amblyopia. Vis. Res. 45, 449–460.
Simmers, A.J., Ledgeway, T., Hess, R.F., McGraw, P.V., 2003. Deficits to global motion processing in human amblyopia. Vis. Res. 43, 729–738.
Simmers, A.J., Ledgeway, T., Mansouri, B., Hutchinson, C.V., Hess, R.F., 2006. The extent of the dorsal extra-striate deficit in amblyopia. Vis. Res. 46, 2571–2580.
Stephan, K.E., Friston, K.J., 2010. Analysing effective connectivity with functional magnetic resonance imaging. Wiley Interdiscip. Rev. Cogn. Sci. 1, 446–459.
Stephan, K., Kasper, L., Harrison, L.M., Daunizeau, J., den Ouden, H.E., Breakspear, M., Friston, K.J., 2008. Nonlinear dynamic causal models for fMRI. Neuroimage 42, 649–662.
Tononi, G., Sporns, O., Edelman, G.M., 1994. A measure for brain complexity: relating functional segregation and integration in the nervous system. Proc. Natl Acad. Sci. USA 91, 5033–5037.
Vaughan, J.T., Adriany, G., Garwood, M., Yacoub, E., Duong, T., DelaBarre, L., Andersen, P., Ugurbil, K., 2002. Detunable transverse electromagnetic (TEM) volume coil for high-field NMR. Magn. Reson. Med. 47, 990–1000.
von Noorden, G.K., Crawford, M.L., 1992. The lateral geniculate nucleus in human strabismic amblyopia. Invest. Ophthal. Vis. Sci. 33, 2729–2732.
Yin, Z.Q., Crewther, S.G., Pirie, B., Crewther, D.P., 1997. Cat-301 immunoreactivity in the lateral geniculate nucleus and visual cortex of the strabismic amblyopic cat. Aust. N Z J. Ophthalmol. 25 (Suppl 1), S107–S109.
Zhu, Q., Billings, S.A., 1996. Fast orthogonal identification of non-linear stochastic models and radial basis function neural networks. Int. J. Control 64, 871–886.